



Lanthanum Chloride Impairs Learning and Memory and Induces Dendritic Spine Abnormality by Down-Regulating Rac1/PAK Signaling Pathway in Hippocampus of Offspring Rats

Wenchang Sun¹ · Jinghua Yang¹ · Yunting Hong¹ · Hui Yuan¹ · Jianbo Wang¹ · Yanqiang Zhang¹ · Xiaobo Lu¹ · Cuihong Jin¹ · Shengwen Wu¹ · Yuan Cai¹

Received: 11 April 2019 / Accepted: 17 October 2019 / Published online: 27 November 2019
© Springer Science+Business Media, LLC, part of Springer Nature 2019

Abstract

Lanthanum (La) is a natural rare earth element. It has neurotoxic effects which can impair learning and memory in humans. However, its mechanism of neurotoxicity is unclear. Learning and memory are coordinated by dendritic spines which form tiny protruding structures on the dendritic branches of neurons. This study investigated the effect of LaCl₃ exposure to pregnant and lactating rats on the offspring rats' learning and memory ability. In this study, rats were divided into 4 groups and given distilled water solution containing 0%, 0.125%, 0.25%, 0.5% LaCl₃, respectively, and this was done from conception to the end of the location. The effects of LaCl₃ on spatial learning and memory ability in offspring rats and in the development of dendritic spines in CA1 pyramidal cells were investigated. The results showed that LaCl₃ impaired spatial learning and memory ability in offspring rats, and decreased dendritic spine density during development. In addition, LaCl₃ can affect the expression of CaMKII, miRNA132, p250GAP, Tiam1, PARD3, and down-regulated the activation of Rac1 which led to a decrease in the expression of Rac1/PAK signaling pathway and downstream regulatory proteins Cortactin and actin-related protein 2/3 complex (Arp2/3 complex). This study indicated that the learning and memory impairment and the decrease of dendritic spine density in the offspring of LaCl₃ exposure may be related to the down-regulation of the Rac1/PAK signaling pathway regulated by Tiam1 and p250GAP.

Keywords Lanthanum · Hippocampus · Learning and memory · Rac1 · Dendritic spine

Wenchang Sun and Jinghua Yang have contributed equally to this work.

Electronic supplementary material The online version of this article (<https://doi.org/10.1007/s10571-019-00748-7>) contains supplementary material, which is available to authorized users.

✉ Jinghua Yang
jhyang@cmu.edu.cn

✉ Yuan Cai
ycai@cmu.edu.cn

¹ Department of Toxicology, School of Public Health, China Medical University, NO.77 Puhe Road, Shenyang North New Area, Shenyang 110122, Liaoning, People's Republic of China

Introduction

Rare earth elements (REEs) are widely found in the natural environment. Examples of REEs include light rare earth elements (LREEs), such as lanthanum (La) and cerium, and heavy rare earth elements (HREEs) such as yttrium and lutecium. These elements have similar chemical properties, exist independently in nature (Consani et al. 2018; Eisenhour and Reisch 2006; Mleczek et al. 2018), have unique physicochemical properties, and are commonly used in agriculture, animal husbandry, aquaculture, medicine, and other fields (Chen et al. 2015; Gwenzi et al. 2018; Wang et al. 2011). China's rare earth reserves are massive and persist in the environment with low mobility. However, REEs can be enriched in food crops and ingested by organisms whereby they bioaccumulate and cause chronic toxicity (Chen and Zhu 2008; d'Aquino et al. 2009). In China, large-scale exploitation of rare earth minerals has led to a sharp increase in the amount of REEs in the environment

ecosystems such as soil and water sources and this greatly affects human health (Miao et al. 2011; Olias et al. 2005; Wen et al. 2006). Therefore, REEs' mechanism of toxicity requires further investigations.

La is a form of LREE, which is chemically active and widely applied in the modern pharmaceutical industry. Epidemiology studies have revealed that REEs induce neurotoxicity in children. This is especially so in children with REEs blood content level 2.18 ± 1.08 ng/g (Fan et al. 2004). Other studies have confirmed that oral administration of 40 mg/kg LaCl_3 in offspring rats for a period of 1–6 months resulted in significant accumulation of La in the brain tissue (Feng et al. 2006). Another study conducted in our group also confirmed that exposure to LaCl_3 during pregnancy to 1 month after weaning resulted in the accumulation of La in the hippocampus and cortex of the brain (Hu et al. 2018; Zhang et al. 2013, 2017a). La has also been shown to cause damage to the offspring rats' nervous system and this leads to abnormalities in the morphology of astrocytes and primary neurons (Sun et al. 2018; Yang et al. 2009; Zhang et al. 2017b). Therefore, La has been used as a representative element for investigating the neurotoxic effects of REEs even though its specific mechanism of toxicity is unclear.

Dendritic spines are the functional micro-protrusions on the dendritic branches of neurons widely found in the mammalian brain tissue. Based on the shape of the spines, they can be subdivided into mushroom, stubby, thin, and branched spines (Bian et al. 2015; Zagrebelsky et al. 2005). Dendritic spines are the original sites of neuronal excitatory synaptic transmission, and their morphology and structure are malleable, leading to changes in synaptic structure and function (Berry and Nedivi 2017; Nishijima et al. 2018). Dendritic spines are associated with learning and memory and studies have shown that the number of mushroom dendritic spines in hippocampal CA1 pyramidal cells is significantly increased after Morris Water Maze training in offspring rats (Beltran-Campos et al. 2011; Joensuu et al. 2018; Luscher et al. 2000). However, mice models of Alzheimer's disease show a significant loss of dendritic spine density in amyloid plaques (Spires et al. 2005; Tsai et al. 2004). Abnormal changes in dendritic spines were also observed in a mouse model of MECP2 duplication syndrome (a children's neurological disease) (Jiang et al. 2013). Also, many neurological diseases and cognitive dysfunction diseases such as Fragile X syndrome, Autism spectrum disorders, and Vascular dementia have been associated with abnormalities in dendritic spines (Grossman et al. 2006; Penzes et al. 2011; Redies et al. 2012; Zoghbi and Bear 2012).

Studies have shown that Ras-related C3 botulinum toxin substrate 1 (Rac1) plays an important role in regulating actin polymerization and dendritic spine plasticity (Haditsch et al. 2009). Chagnon showed that Rho GTPase-activating protein 32 (p250GAP) was an important GAP

which negatively regulated Rac1 activation and affects Rac1-induced regulation of the growth and plasticity of dendritic spines (Chagnon et al. 2010). T-lymphoma invasion and metastasis 1 (Tiam1) plays an important role in regulating the plasticity of hippocampal dendritic spines and this requires the involvement of partitioning defective 3 (PAR3). Besides, Rac1 directly activates the P21-activated kinase (PAK) to regulate actin polymerization and remodeling, which in turn affects the dendritic spine plasticity (Wegner et al. 2008). Therefore, this study investigated the relationship between learning and memory impairment and dendritic spine injury in hippocampal pyramidal neurons of offspring rats treated with LaCl_3 , and explored the underlying mechanism from the perspective of the Rac1/PAK signaling pathway regulated by Tiam1 and p250GAP.

Materials and Methods

Animals

Sixty-four Wistar rats, (30 males and 30 females, weight 230 ± 20 g, license number: SCXK- 2013-0001) were obtained from the Experimental Animal Center of China Medical University. The rats were housed in a standard environment (temperature 23 ± 1 °C, humidity $55 \pm 5\%$, with 12-h light/12-h dark daily), and allowed to eat standard food and drink water ad libitum. Animals were acclimatized for 1 week before use in experiments. Female Wistar rats were randomly divided into four groups, including control group, 0.125% LaCl_3 group, 0.25% LaCl_3 group, and 0.5% LaCl_3 group (calculated by weight equivalent to 0 mg/kg, 125 mg/kg, 250 mg/kg, 500 mg/kg LaCl_3) (Hu et al. 2018; Zhu et al. 1997). Female and male rats were mated in the same cage ($\text{♀}/\text{♂} = 1:1$). The day when sperms were detected in the vaginal plug and the vaginal discharge was recorded as day 0 of pregnancy. The pregnant rats were individually housed and exposed to an aqueous distilled solution containing LaCl_3 (Sinopharm Chemical Reagent Co., Ltd.) containing one of the following four doses, 0, 0.125% LaCl_3 , 0.25% LaCl_3 , 0.5% LaCl_3 , respectively. The birth of the pups was defined as postnatal day 0 (PND 0). For offspring rats, La^{3+} was mainly ingested through the placenta and milk, and the poisoning was terminated on PND 20. On PND 0, 8 pups were randomly retained in each group. All experiments and surgical procedures were approved by the Institutional Animal Care and Use Committee of China Medical University, and complied with the National Institute of Health Guide for the Care and Use of Laboratory Animals. All efforts were made to minimize the number and suffering of animals used.

Morris Water Maze

The Morris water maze (MWM) is a common laboratory tool for investigating spatial learning and memory abilities of laboratory rats in neuroscience. The water maze consists of a circular pool with black circumference and bottom (diameter of 150 cm and height of 60 cm, 30 cm depth of water and maintained at 25 ± 1 °C). The pool had four quadrants. In the center of the second quadrant, there is a platform (15 cm in diameter) hidden about 2 cm below the surface of the water. On PND 21, one pup was randomly selected from each litter for experimentation. A total of 32 rats (male or female), with 8 rats in each group, were selected. During the experiment, the rats in each dose group were assigned into 2 cages, with 4 rats per cage, allowing them to freely consume and drink distilled water. During the training, the rat's head was positioned in the water pool at the center of each quadrant, and allowed to swim freely for 60 s to find the underwater platform. If the rats found the platform, they were allowed to rest on the platform for 20 s. If they failed to find it, we guided the rats to the platform and allowed them to rest for 20 s. Each rat was trained four times a day (one quadrant per day) for 5 days. After the training, the rats rested for 1 week and were utilized for place navigation test and exploration test.

First, the rats were utilized for place navigation test. The experimental conditions were similar to those of the training period. Escape latency was recorded and analyzed while the rat was looking for the underwater platform. At the end of the place navigation test, the underwater platform was removed and the spatial exploration test was performed. The rats were permitted to swim for 60 s after being placed in the pool, and their memory capacity was evaluated according to the number of times they entered the second quadrant and passed through the platform. During the test, the rats were tested every day at the same time to avoid the influence of the physiological changes at different times on the experimental results. The swimming search strategy for the rats was recorded and analyzed using the EthoVision XT 11.5 system (Noldus, Netherlands).

Golgi-Cox Staining

Golgi-Cox impregnation is among the most effective techniques for studying normal and abnormal morphology of neurons and glial cells. In this study, the FD Rapid GolgiStain Kit (FD NeuroTechnologies, Inc, USA) was used to analyze the changes of dendritic spines in the hippocampal CA1 region of pups exposed to LaCl_3 . Rats were anesthetized and the brain was removed immediately, but carefully to avoid damaging or squeezing the tissue. The brain was sliced with a sharp blade into blocks

of approximately 10 mm thicknesses (adjusted to ensure that the hippocampus formation was complete). The tissue was immersed in pre-prepared liquid mixture, and the new liquid was replaced the next day and stored at room temperature for 2 weeks in a dark environment. Next, the tissue was transferred to solution C provided in the kit, and the solution was replaced with a new liquid the next day, after which the tissue was immersed in the solution in the dark at room temperature for 3 days. The tissue was rapidly frozen with isopentane and temporarily stored on dry ice. This was followed by cutting the tissue into 100 μm slices at -25 °C using a cryostat, and slices were collected with gelatin-coated slides, and dried at room temperature in the dark. The tissue slices were stained in accordance with instructions of the kit. The slices were washed with Milli-Q water, soaked in a liquid mixture, dehydrated with gradient alcohol, dewaxed with xylene, sealed with resin, and examined after drying.

The slices were observed under a $\times 1000$ optical microscope (Leica DM500, Germany). Neurons were included in the analysis only if they were intact, fully impregnated, and could not be obscured with stain precipitations. The density of dendritic spines was quantified by selecting 10 well-defined dendritic segments of CA1 pyramidal neurons in each section by random sampling. Four slices were taken from each dose group, and each slice was from different litters of pups. Statistical analysis was performed using ImageJ software. Dendritic spine density was expressed as the number of spines on the dendrites per 10 μm length. Total spines and spines of various types were analyzed separately. Morphology of spines was defined as stubby, mushroom, thin, and branched. The data processor was blinded to the processing conditions.

Rac1 Pull-Down Assay

Experiments were performed using Rac1 Activation Magnetic Beads Pull-down Assay (Milipore, USA). Tissues from the hippocampal CA1 area were carefully isolated and frozen rapidly in liquid nitrogen. After the addition of ice-cold Mg^{2+} Lysis/Wash Buffer (MLB), the hippocampus tissue was lysed and the tissue lysates collected. Active GTPase Binding Domain (PBD) is a downstream target of activated GTPase-GTP. Pak1 PBD is a fusion of GST coupled to glutathione-magnetic beads pulled down to bind GTP-Rac1 in tissue lysate extract. The reaction mixture was incubated for 45 min at 4 °C. The beads were gathered and washed with MLB. The agarose was re-suspended in $2 \times \text{Laemmli}$ and boiled for 5 min. Western blot was used to quantify the expression of GTP-Rac1 in the samples using the Rac1 monoclonal antibody.

RNA Isolation and Real-Time PCR

After the offspring rats were anesthetized, the hippocampus tissues were isolated and stored in -80°C refrigerator. Tissue RNA extraction was performed using the GeneJET RNA Purification Kit (Thermo Fisher, USA) according to the manufacturer's protocol. RNA concentrations were measured using Nanodrop (Thermo Fisher, USA) and the concentration was equalized among the groups. cDNA was synthesized by reverse transcription using the PrimeScript RT kit (Takara, Dalian, China) according to the manufacturer's protocol. Real-time PCR amplification reactions were performed by SYBR Premix Ex TaqII (Takara, Dalian, China) and LightCycler 480 (Roche, Switzerland). Primer sequence design and synthesis were performed by Takara. The primer sequences are shown in Table 1 and Gapdh as the internal reference. The miRNA132 primer was designed and tested using the Bulge-LoopTM miRNA qRT-PCR Primer kit and U6 (Ribobio, China) as the internal reference. The results were quantified using the $2^{-\Delta\Delta\text{Ct}}$ method.

Western Blotting

The hippocampus tissue of the anesthetized offspring rats was carefully isolated and stored in a -80°C refrigerator. Tissue samples from the hippocampal CA1 region were prepared into tissue extracts using RIPA, PMSF (Dingguo Changsheng, China), and protease inhibitors (Beyotime, China). The BCA kit (Dingguo Changsheng, China) was

used for protein quantification. The protein samples were denatured by boiling after quantification and cooling on ice. The target protein was separated using 6–10% SDS-PAGE gel electrophoresis, 80 V 30 min, 110 V 60 min and transfer to the PVDF membrane after the gel was done, and then the PVDF membrane was placed in TBST containing 5% skim milk powder for 2 h at room temperature. The PVDF membrane was then probed overnight at 4°C according to the following antibody concentrations: CaMKII (1:1000, Absin, China), Tiam1 (1:500, Santa Cruz, USA), PARD3 (1:1000, Thermo Fisher, USA), Rac1 (1:1000, Abcam, USA), PAK1/2/3 (1:1000, US Science and Technology Commission), p-PAK1/2/3 (1:1000, China Bioss), Cortactin (1:1000, US Science and Technology Commission), Arp2/3 Complex Subunit 1B (1:1000, Novus Corporation, USA), and GAPDH (1:3000, Proteintech, USA). The next day, the PVDF membrane was washed 4 times with TBST, each time 10 min. The PVDF membrane was incubated for 1.5 h with HRP Goat Anti-Rabbit IgG (H + L) (1:3000, ABClonal, China) and horseradish-labeled goat anti-mouse IgG (1:3000, Dinguo Changsheng, China) at room temperature. The membrane was washed 4 times for 10 min. A hypersensitive ECL chemiluminescence kit (Beyotime, China) was used to visualize the strip in a fully automated chemiluminescence image analysis system (Tanon 5200, China). Protein expression was analyzed using ImageJ with GAPDH serving as an internal reference. The integrated density value (IDV) was used to indicate the expression level of the protein.

Table 1 Primer sequence of the target gene

Gens	Accession number	Primer sequences (5'–3')
<i>Camk2a</i>	NM_012920.1	Forward: -ATGCTGCCAAGATTATCAACACCA- Reverse: -GTGCTTCAACAAGCGGCAGA-
<i>Arhgap32</i>	XM_017595999.1	Forward: -GCAAGCCATAGGCAGTTATGTGAG- Reverse: -CAACTCTATTGCTCCCGGGGCTC-
<i>Tiam1</i>	NM_001100558.1	Forward: -GTCCGAAAGTCACCGAGAATC- Reverse: -GAACGCCATCTTCGTCCACA-
<i>Pard3</i>	NM_031235.1	Forward: -CCGTACCTACAGCTTTGAGCAATC- Reverse: -CGCTGCACTTGAACCTCCAC-
<i>Rac1</i>	NM_134366.1	Forward: -CCTGCTCATGTTACACGACCA- Reverse: -GTCCCAGAGGCCAGATTCA-
<i>Pak1</i>	NM_017198.1	Forward: -ACAGGCTGTTCTGGATGTGTTG- Reverse: -TGACACTGGTGGCACTGCTG-
<i>Pak2</i>	NM_053306.3	Forward: -CATGGCTATCGAAATGGTGGAAAG- Reverse: -GCTCAGGTGTTCCATTCGTTG-
<i>Pak3</i>	NM_019210.1	Forward: -CCATGGATATATAGCAGCACATCAG- Reverse: -TGGTCTTGGTGAATGACAGG
<i>Cttm</i>	NM_021868.2	Forward: -ATCGTCACAGATGCCCTCACA- Reverse: -CACAGCATGGCCTGCAGAA
<i>Arpc2</i>	NM_001106919.1	Forward: -TCCGGACTATCTGCACTACCA- Reverse: -TCCCAAGAGTTAGCGGGATGA-
<i>Gapdh</i>	NM_017008.3	Forward: -GGCACAGTCAAGGCTGAGAATG- Reverse: -ATGGTGGTGAAGACGCCAGTA-

Immunohistochemistry and Immunofluorescence

Normal saline and 4% paraformaldehyde were perfused into the brain of anesthetized offspring rat and the brain tissue was then separated and fixed in paraformaldehyde for 1 week. Dehydration of the tissue by gradient alcohol was done and paraffin slices were made transparent using xylene. The tissue wax block was cut into 5- μ m-thick slices using a slicer. The slices were dried and baked at 58 °C for 2 h and stored at room temperature for use in subsequent experiments.

1. Immunohistochemistry was utilized to detect the expression of p250GAP. The experiments were performed following the manufacturer's protocol (MXB, MXB Biotechnologies, China). Slices were dewaxed using xylene, hydrated by gradient alcohol, washed with PBS, and incubated in sequence using peroxidase blocker and normal goat non-immune serum for 10 min at room temperature. p250GAP antibody (1:300, Absin, China) was added and incubated for 1 h at room temperature and overnight at 4 °C. The following day the slices were warmed at 37 °C for 30 min, and the primary antibody was removed. Biotin-labeled secondary antibody and streptavidin-peroxidase solution were added dropwise, and each was stored at room temperature for 10 min. DAB (MXB Biotechnologies, China) was added for 5 min and counterstained using hematoxylin nucleus for 1 min, soaked in 1% hydrochloric acid alcohol and for several seconds and differentiated the nuclei using water for 10 min. The slices were dehydrated with gradient alcohol and sealed using resin. Images were observed using an optical microscope (Leica DM500, Germany).

2. The expression of Tiam1 and PARD3 was observed by immunofluorescence staining. The slices were dewaxed and hydrated, and after EDTA (Beyotime, China) antigen retrieval, 0.3% Triton X-100 was used to permeabilize for 12 min. The samples were washed 3 times using PBS for 5 min, and blocking was achieved using 5% BSA at room temperature for 60 min. Rabbit anti-PARD3 (1:50, Thermo Fisher, USA) and mouse anti-Tiam1 (1:50, Santa Cruz, USA) were added dropwise for 1 h at room temperature and left overnight at 4 °C. The following day, the slices were warmed at 37 °C for 30 min, and then washed with PBS in the dark. FITC-labeled goat anti-rabbit (green) and Cy3-labeled goat anti-mouse (red) were added in the dark for 1 h. After washing and staining with DAPI (Beyotime, China) for 5 min, mounting was done, using anti-fluorescence. The image was immediately observed under a fluorescence microscope (Nikon 80i, Japan).

The co-localization coefficients of red and green fluorescence of each image were analyzed using Image-Pro Plus image processing software (Media Cybernetics, USA), and Pearson's correlation coefficient was used as the co-localization the coefficients of each image for statistical analysis.

Statistics Analysis

All experimental data were expressed as mean \pm the standard deviation (SD), and the error bars on the graphs represented the SD. All data were statistically analyzed using SPSS Software version 19.0 (SPSS Inc., IBM, USA). One offspring rat was randomly selected from each litter for the water maze test. For other experiments, at least 3 litters were randomly selected in each dose group, and 1 offspring rat was randomly selected from each litter for 3 independent experiments. The *n* in the results indicates the number of animals that were repeated. Escape latency data were analyzed by ANOVA for the repeated measures. After Mauchly's test of sphericity was used to judge the data correlation $P < 0.05$, the differences were analyzed by LSD test. Other data were analyzed using one-way analysis of variance (one-way ANOVA) to find the differences between the groups. When the *F* value was statistically significant, the SNK test was used for post hoc testing. $P < 0.05$ was regarded as statistically significant.

Results

Effect of LaCl₃ on Spatial Learning and Memory Ability in Offspring Rats

The training results of the offspring rats are illustrated in Fig. 1a. On the 1st day of training, most of the pups in each group swam without a target and only a few could find the underwater platform. From the 2nd day of training, some pups could find the underwater platform. As the number of training days increased, the number of pups finding the underwater platform increased and the escape latency gradually decreased. By the 5th day of the training, all pups could find the underwater platform and the escape latency was significantly shortened compared to the initial training day. The escape latency of each group of pups on the same day was also statistically analyzed. However, on the 3rd and 4th day of training the escape latency of the LaCl₃ exposed group looking for an underwater platform was statistically significant compared to the control group ($P_{\text{Day}3} = 0.893$, $P_{\text{Day}4} = 0.966$). By the 5th day of training, there was no significant difference in escape latency between the groups looking for underwater platforms ($P = 0.896$).

After 5 days of training, the offspring rats were maintained for 1 week and tested for place navigation. The results showed that the escape latency of offspring rats looking for underwater platforms was high due to an increase in LaCl₃ exposure dose. Compared with the control group, the escape latency of 0.125%, 0.25%, and 0.5% LaCl₃ groups was significantly increased (Fig. 1b, $F_{(3,28)} = 20.404$, $P = 0.001$). The trajectory heat map of

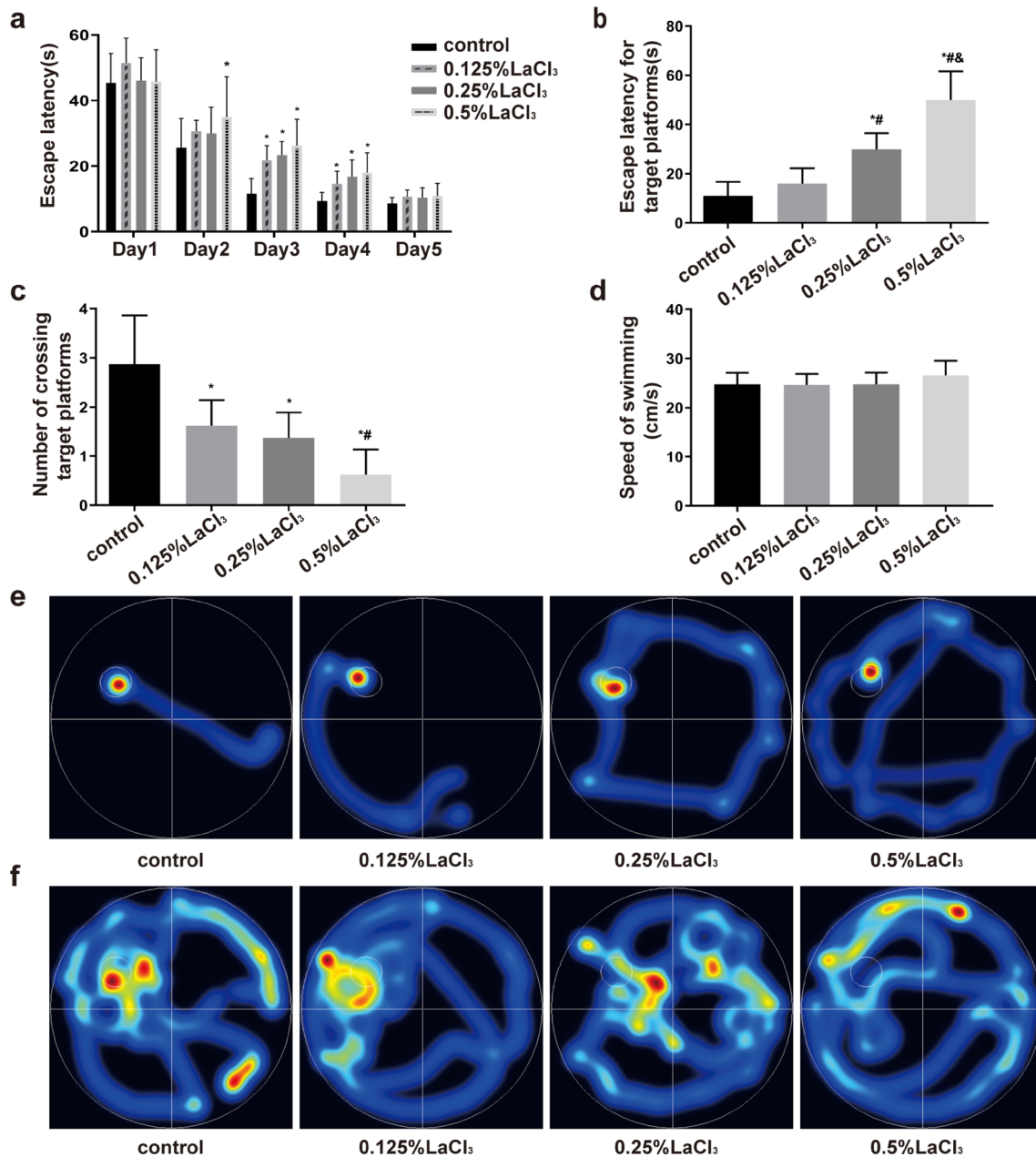


Fig. 1 Effect of LaCl₃ on spatial learning and memory in the MWM test. **a** Results of the first 5 days of training in each group of offspring rats. **b, e** The escape latency of LaCl₃-treated offspring rats and representative trajectory heat map for searching platform in the place navigation test. **c, f** Number of crossing target platform of LaCl₃-treated offspring rats and representative trajectory heat map in the spatial

exploration experiment. **d** Effect of LaCl₃ on swimming speed of offspring rats. The bar graph represented $\bar{X} \pm SD$ ($n = 8$, number of animals). Compared with the control group, * $P < 0.05$; compared with the 0.125% LaCl₃-treated group, # $P < 0.05$; compared with the 0.25% LaCl₃-treated group, & $P < 0.05$

each group looking for the underwater platform latency indicated that the control group directly and quickly found the underwater platform. With an increase in LaCl₃ dose, the trajectory of the LaCl₃ exposed the offspring rats looking for the underwater platform was disorganized, aimless, and the escape latency increased. Some pups of the 0.5% LaCl₃ group could not find the underwater

platform (Fig. 1e). After place navigation test was completed, the hidden underwater platform was removed and a spatial exploration test was carried out. The results showed that the control offspring rats repeatedly traversed at the position of the target platform. Increased doses of LaCl₃ decreased the number of passages of each group of offspring rats passing through the underwater

platform. The 0.5% LaCl_3 group did not make it to the underwater platform position. The control group was statistically different from each of the LaCl_3 groups (Fig. 1c, $F_{(3,28)} = 16.193$, $P < 0.001$). This indicated that LaCl_3 exposure impaired spatial learning and memory ability of offspring rats. However, analysis of swimming speed showed that administration of LaCl_3 did not affect the exercise ability of the offspring as compared to offspring rats of control group (Fig. 1d, $F_{(3,28)} = 1.120$, $P = 0.3577$).

Effect of LaCl_3 on the Dendritic Spines in Pyramidal Neurons of Hippocampal CA1 Region in Offspring Rats

The dendritic spine density of the pyramidal neurons in the hippocampal CA1 region of the offspring rats was measured by Golgi-Cox staining (Fig. 2a–d). The study results showed that the dendritic spine density declined with an increase in LaCl_3 dosage (Fig. 2e). The 0.25%, 0.5% LaCl_3 treatment group was statistically significant compared to

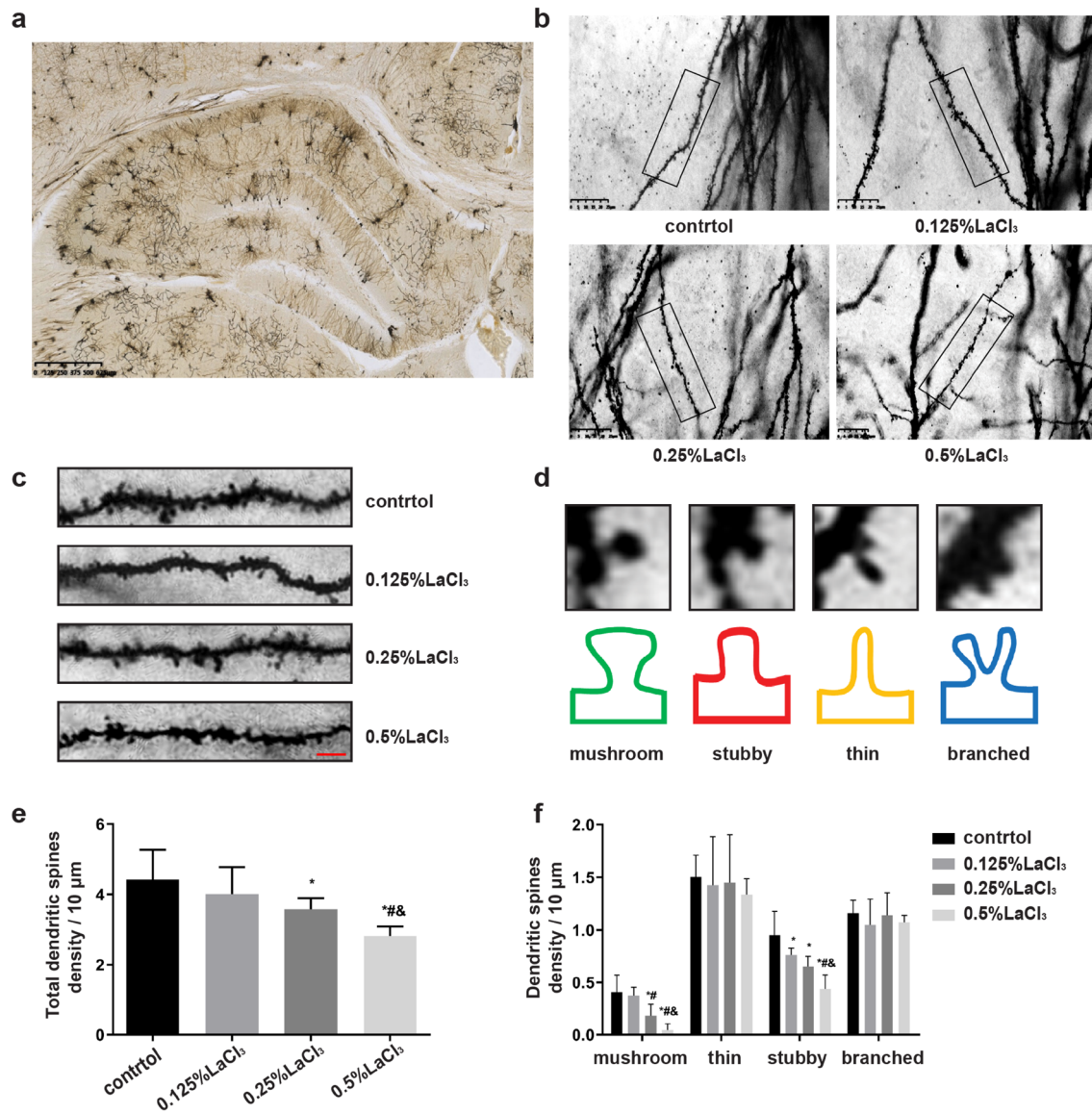


Fig. 2 Effect of LaCl_3 on the dendritic spines in pyramidal neurons of hippocampal CA1 region of offspring rats. **a** Schematic diagram of the structure of the hippocampus stained by Golgi-Cox. **b, c** The dendritic spines in pyramidal neurons of hippocampal CA1 region in offspring rats neurons. **d** Different types of dendritic spines. **e** Total dendritic spine density in pyramidal neurons of hippocampal CA1

region in offspring rats. **f** The density of various types of dendritic spines in pyramidal neurons of hippocampal CA1 region in offspring rats. The bar graph represented $\bar{X} \pm SD$ ($n = 4$, number of animals). Scale bar = 5 μm . Compared with the control group, * $P < 0.05$; compared with the 0.125% LaCl_3 -treated group, # $P < 0.05$; compared with the 0.25% LaCl_3 -treated group, & $P < 0.05$

the control group [$F_{(3,12)} = 10.133$, $P = 0.0019$]. In addition, analysis of different types of dendritic spines found that the density of mushroom and stubby dendritic spines decreased with increasing LaCl_3 treatment, and the 0.25%, 0.5% LaCl_3 treatment groups were statistically different from the control group [$F_{\text{mushroom}(3,12)} = 16.752$, $F_{\text{stubby}(3,12)} = 13.108$, $P < 0.001$]. LaCl_3 treatment had no significant effect on the density of thin and branched dendritic spines [Fig. 2f, $F_{\text{thin}(3,12)} = 1.52$, $P = 0.24$, $F_{\text{branched}(3,12)} = 0.386$, $P = 0.765$].

Effect of LaCl_3 on the Expression of microRNA132 and p250GAP in the Hippocampus of Offspring Rats

The expression levels of microRNA132 and p250GAP in the hippocampus of the offspring rats are presented in Fig. 3. The transcript level of miRNA132 in the hippocampus of LaCl_3 -treated offspring rats decreased significantly compared to the control group (Fig. 3a, $F_{(3,8)} = 15.822$, $P = 0.001$). The transcription level of p250GAP gene *Arhgap32* in the hippocampus of LaCl_3 -treated offspring rats increased significantly compared to the control group

(Fig. 3b, $F_{(3,8)} = 34.434$, $P < 0.001$). The immunohistochemistry results matched the real-time PCR results, and the expression level of p250GAP protein in the hippocampus of LaCl_3 -treated offspring rats increased significantly compared to the control group [Fig. 3c, d, $F_{(3,8)} = 10.809$, $P = 0.003$].

Effect of LaCl_3 on the Expression of CaMKII, Tiam1, and PARD3 in the Hippocampus of Offspring Rats

Figure 4 shows that in comparison with the control group, transcriptional levels of *Camk2a*, *Tiam1*, and *Pard3* mRNA decreased with an increase in LaCl_3 exposure [Fig. 4a, d, g, $F_{\text{Camk2a}(3,8)} = 13.545$, $P = 0.002$, $F_{\text{Tiam1}(3,8)} = 14.803$, $P = 0.003$, $F_{\text{Pard3}(3,8)} = 30.041$, $P < 0.001$]. The western blot results were consistent with changes in the mRNA levels. The expression levels of CaMKII, Tiam1, and PARD3 were negatively correlated with the exposure level of LaCl_3 in comparison to the control group [Fig. 4(b, c), (e, f), (h, i), $F_{\text{CaMKII}(3,8)} = 25.406$, $P < 0.001$, $F_{\text{Tiam1}(3,8)} = 17.916$, $P < 0.001$, $F_{\text{PARD3}(3,8)} = 31.206$, $P < 0.001$]. The immunofluorescence double staining results showed that the

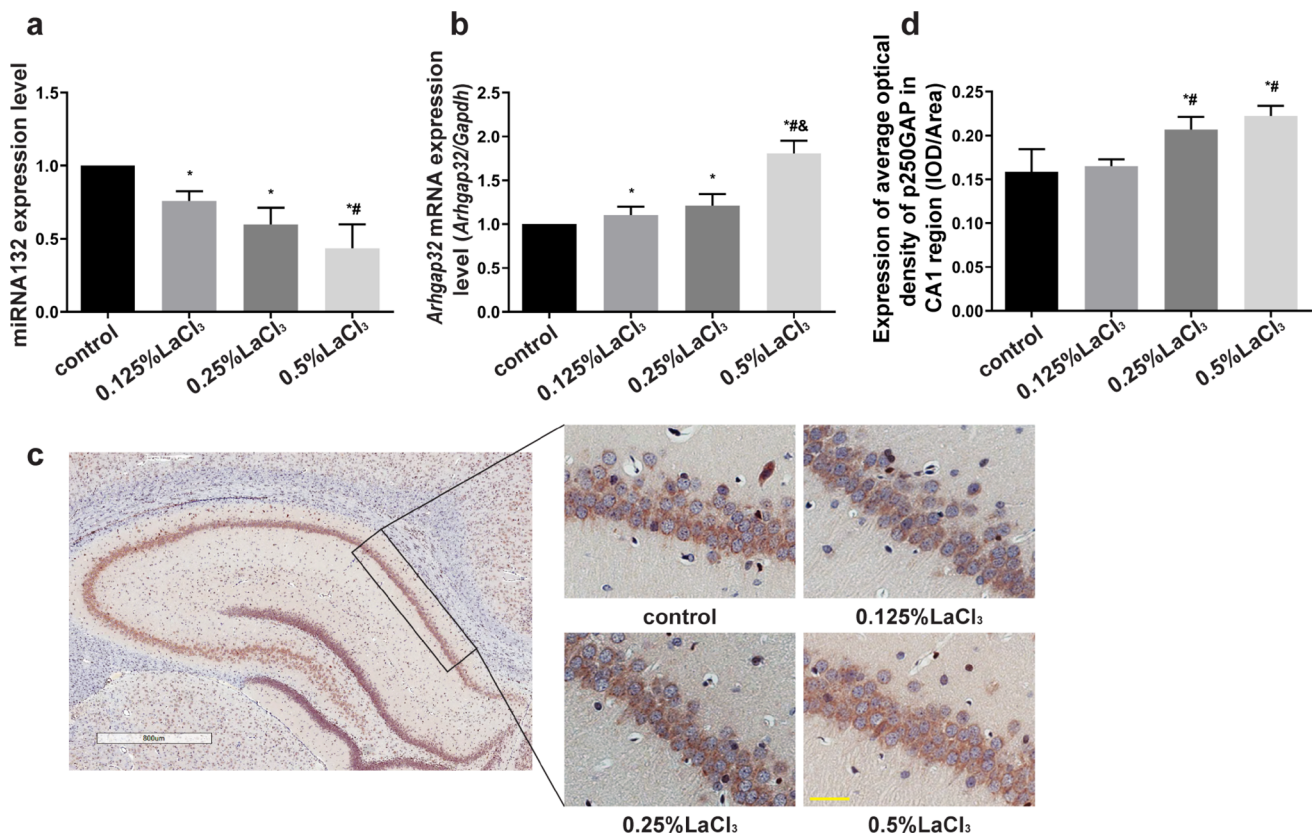


Fig. 3 Effect of LaCl_3 on the expression of miRNA132 and p250GAP in hippocampus of offspring rats. **a** Transcript level of microRNA132 in the hippocampus of offspring rats. **b** *Arhgap32* mRNA transcription level in the hippocampus of offspring rats. **c, d** Immunohistochemistry results of p250GAP in hippocampal CA1 region

of offspring rats. The bar graph represents $\bar{X} \pm SD$ ($n = 3$, number of animals). Scale bar = 20 μm . Compared with the control group, * $P < 0.05$; compared with the 0.125% LaCl_3 -treated group, # $P < 0.05$; compared with the 0.25% LaCl_3 -treated group, & $P < 0.05$

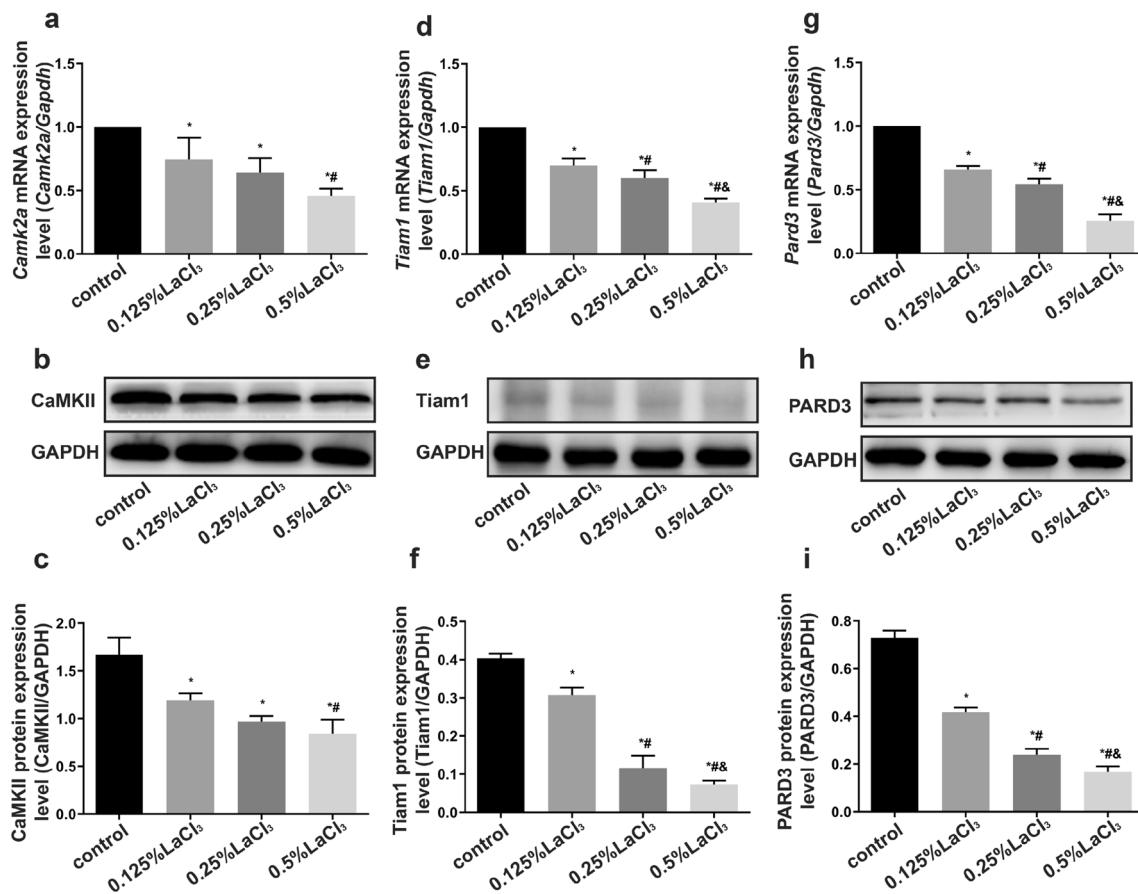


Fig. 4 Effect of LaCl_3 on the expression of CaMKII, Tiam1, and PARD3 in hippocampus of offspring rats. **a** *Camk2a* mRNA transcription in the hippocampus of offspring rats. **b** CaMKII western blot results. **c** CaMKII protein expression levels. **d** *Tiam1* mRNA transcription in the hippocampus of offspring rats. **e** Tiam1 western blot results. **f** Tiam1 protein expression levels. **g** *Pard3* mRNA tran-

scription in the hippocampus of offspring rats. **h** PARD3 western blot results. **i** PARD3 protein expression levels. The bar graph represents $\bar{X} \pm SD$ ($n = 3$, number of animals). Compared with the control group, * $P < 0.05$; compared with the 0.125% LaCl_3 -treated group, # $P < 0.05$; compared with the 0.25% LaCl_3 -treated group, & $P < 0.05$

expression of Tiam1 and PARD3 decreased with an increase in LaCl_3 dosage [Fig. 5a–c, $F_{\text{Tiam1}(3,8)} = 10.921$, $P = 0.003$, $F_{\text{PARD3}(3,8)} = 7.411$, $P = 0.005$]. Tiam1 plays a role in regulating dendritic spine plasticity and requires the participation of PARD3. Co-localization analysis showed that the coefficient of Tiam1 and PARD3 was not related to the exposure [Fig. 5d, $F_{(3,8)} = 0.386$, $P = 0.765$].

Effect of LaCl_3 on Rac1 Activity in the Hippocampus of Offspring Rats

To investigate the mechanism of the effects of LaCl_3 on dendritic spine plasticity, the expression of total Rac1 and GTP-Rac1 was determined (Fig. 6). The results showed that the transcription of *Rac1* mRNA decreased with an increase in LaCl_3 dosage [Fig. 6a, $F_{(3,8)} = 48.558$, $P < 0.001$], and the total Rac1 expression decreased gradually (Fig. 6c, $F = 49.36$, $P < 0.001$). The expression of GTP-Rac1 by Pull-down assay showed that an increase in LaCl_3 exposure

down-regulated the expression of GTP-Rac1 [Fig. 6d, $F_{(3,8)} = 113.296$, $P < 0.001$].

Effect of LaCl_3 on the Expression of PAK, Cortactin, and Arp2/3 Complex in the Hippocampus of Offspring Rats

Figure 7 shows the results. The transcriptional expression of PAK-major subtypes *Pak1*, *Pak2*, and *Pak3* mRNA was detected since it possesses multiple subtypes [Fig. 7a–c, o, $F_{\text{Pak1}(3,8)} = 30.488$, $P < 0.001$, $F_{\text{Pak2}(3,8)} = 29.982$, $P < 0.001$, $F_{\text{Pak3}(3,8)} = 19.286$, $P < 0.001$]. PAK protein expression level was not associated with LaCl_3 treatment, while p-PAK expression decreased with increased LaCl_3 exposure [Fig. 7d–f, $F_{\text{p-PAK}(3,8)} = 28.952$, $P < 0.001$]. The transcription levels of *Cttn* and *Arpc2* mRNA were detected by real-time PCR. The transcription of *Cttn* and *Arpc2* mRNA decreased with an increase of LaCl_3 exposure compared to the control [Fig. 7g, j, $F_{\text{Cttn}(3,8)} = 31.402$,

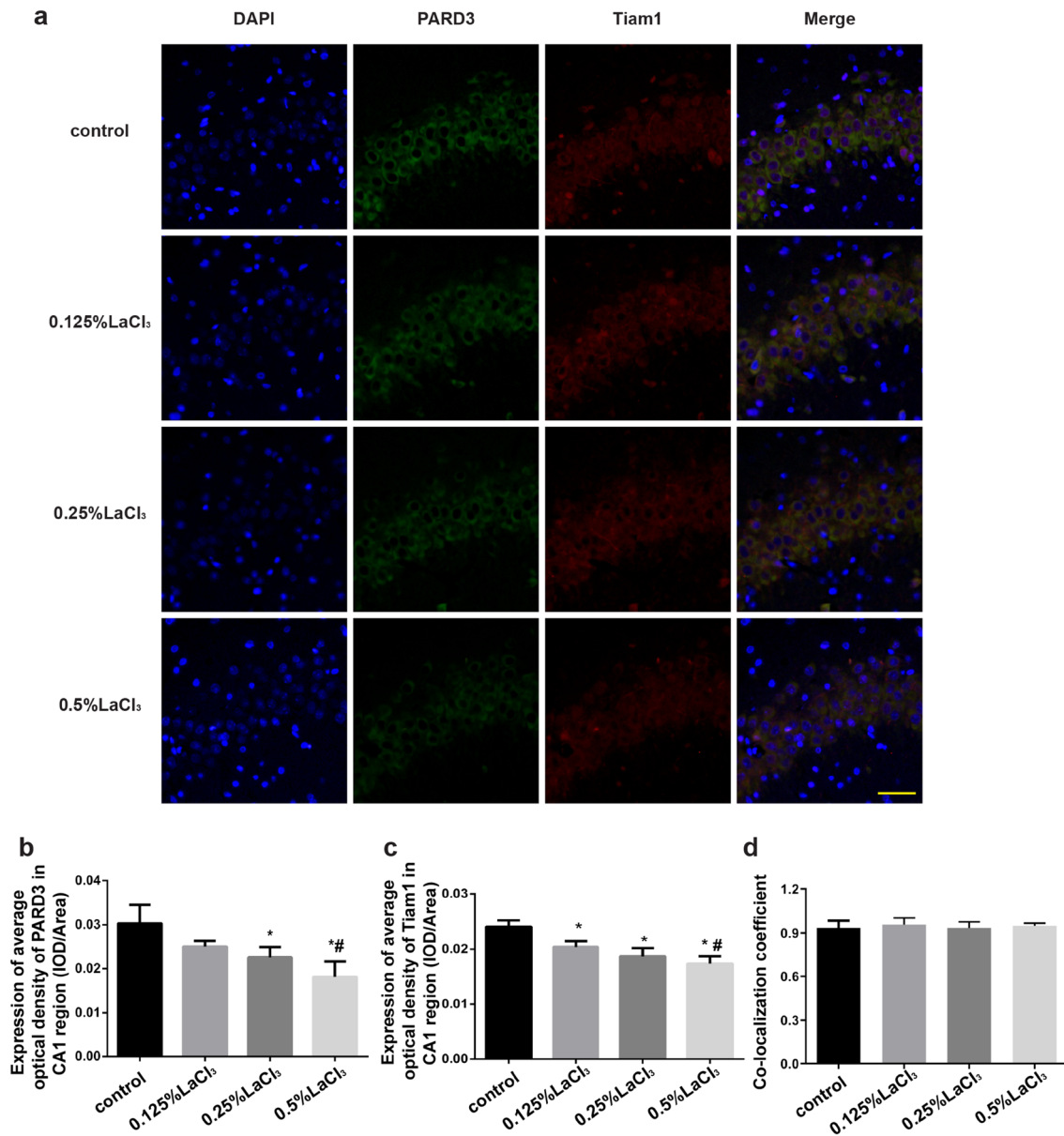


Fig. 5 Effect of LaCl₃ on co-localization of Tiam1, and PARD3 in hippocampus of offspring rats. **a** Tiam1, PARD3 immunofluorescence double-stained picture. **b** PARD3 immunofluorescence expression level. **c** Tiam1 immunofluorescence expression level. **d** Fluorescence

co-localization analysis of Tiam1 PARD3. The bar graph represents $\bar{X} \pm SD$ ($n=3$, number of animals). Scale bar=20 μm . Compared with the control group, * $P < 0.05$; compared with the 0.125% LaCl₃-treated group, # $P < 0.05$

$P < 0.001$, $F_{Arpc2(3,8)} = 86.734$, $P < 0.001$]. Examination of the expression levels of Cortactin and the main subtype of Arp2/3 complex subunit 1B of Arp2/3 complex showed that the expression levels of the two proteins were reduced with an increase in LaCl₃ dosage [Fig. 7(h, i), (k, l), $F_{Cortactin(3,8)} = 69.86$, $P < 0.001$, $F_{Arp2/3\text{complexsubunit1B}(3,8)} = 21.094$, $P < 0.001$].

Discussion

Exposure to and REEs intake exert adverse effects on human health. Previous studies have shown that REEs ingestion can cause accumulation in various organ tissues and exhibit an uneven distribution (Allison et al. 2015;

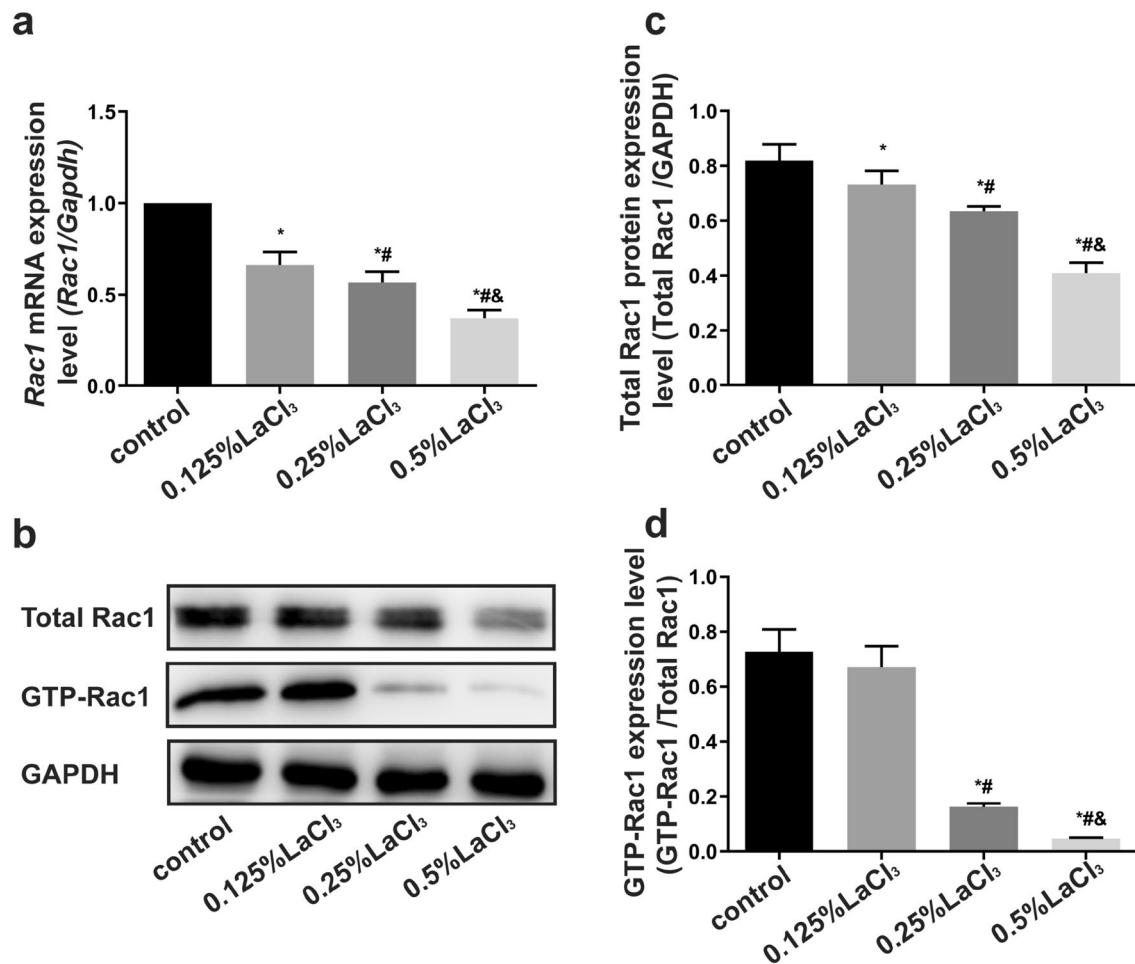


Fig. 6 Effect of LaCl₃ on the expression of Rac1 and GTP-Rac1 in hippocampus of offspring rats. **a** Transcript level of *Rac1* mRNA in hippocampus of rats. **b–d** Total Rac1 and GTP-Rac1 expression levels in the hippocampus of the pups. The bar graph represents

$\bar{X} \pm SD$ ($n=3$, number of animals). Compared with the control group, * $P < 0.05$; compared with the 0.125% LaCl₃-treated group, # $P < 0.05$; compared with the 0.25% LaCl₃-treated group, & $P < 0.05$

Rainbow 2007). Other studies have shown that exposure of pregnant rats to LaCl₃ by gavage feeding from the onset of pregnancy to 6 months after weaning of the offspring increased La content in the blood, hippocampus, and cortex of the offspring in a dose-dependent manner (He et al. 2008). This suggests that La accumulates in the hippocampus and causes its toxic effect.

The MWM test is a classic approach used to identify spatial learning and memory ability in rats (D’Hooge and De Deyn 2001). In this study, maternal rats were fed with an aqueous solution containing LaCl₃ during pregnancy and lactation. MWM in the offspring rats was carried out after weaning to verify that the animal model had been built successfully. The results showed that when looking for the underwater platform on the 3rd and 4th days of training, the offspring rats with La treatment showed weaker learning ability than those in the control group. In subsequent place navigation tests and spatial exploration tests, the learning

and memory ability of LaCl₃-treated groups gradually decreased with increasing LaCl₃ dosage. These results confirmed that maternal exposure to LaCl₃ during pregnancy and lactation impaired spatial learning and memory ability of offspring rats.

It is well known that the hippocampus is an important brain area responsible for performing learning and memory functions in the CNS. Dendritic spines are the original sites of excitatory synaptic transmission in the central nervous system, which are closely related to information acquisition and storage. Dendritic spines are abundant in hippocampal neurons, and their morphology, number, and distribution display significant plasticity and determine the synaptic structure and function (Greenhill et al. 2015; Ota et al. 2013; Sala and Segal 2014). Studies have shown that changes in dendritic spine density and structure are crucial for post-synaptic plasticity and contribute to the morphological basis of learning and memory function (Dumitriu et al. 2010;

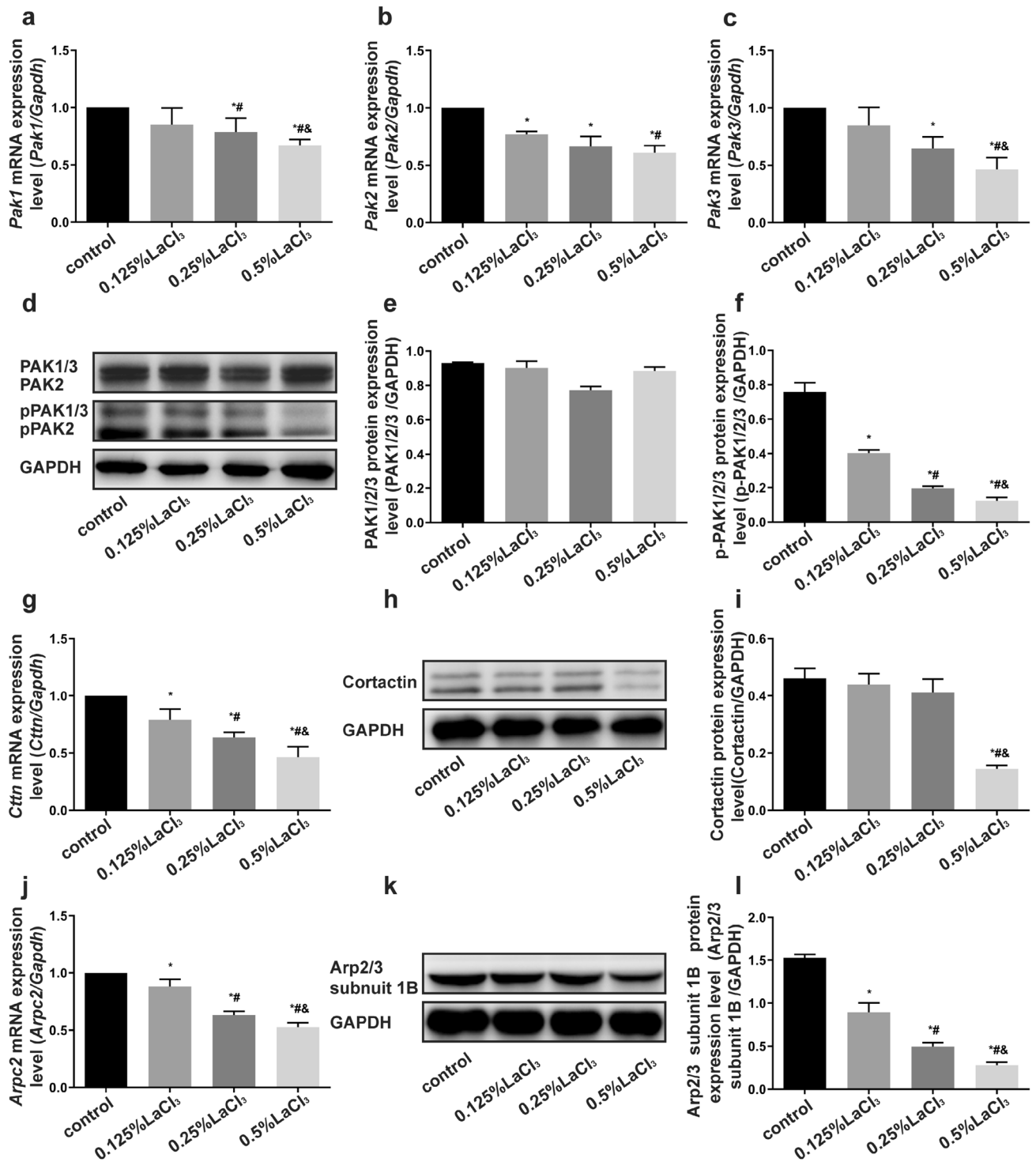


Fig. 7 Effect of LaCl₃ on the expression of PAK, Cortactin, and Arp2/3 complex in hippocampus of offspring rats. **a–c** *Pak1*, *Pak2*, and *Pak3* mRNA transcription level in the hippocampus of offspring rats. **d** PAK, p-PAK protein western bolt results. **e** PAK protein expression level. **f** p-PAK protein expression level. **g** *Cctn* mRNA transcription level in hippocampus of offspring rats. **h** Western blot results of Cortactin protein. **i** Cortactin protein expression levels. **j**

Arpc2 mRNA transcription level in hippocampus of offspring rats. **k** Western blot results of Arp2/3 complex subunit 1B protein. **l** Arp2/3 complex subunit 1B protein expression level. The bar graph represents $\bar{X} \pm SD$ ($n=3$, number of animals). Compared with the control group, * $P < 0.05$; compared with the 0.125% LaCl₃-treated group, # $P < 0.05$; compared with the 0.25% LaCl₃-treated group, & $P < 0.05$

Zhao et al. 2018). Previous studies have indicated that the number of dendritic spines in mice increases rapidly after birth, reaching the apex at puberty after which it gradually decreases (Bian et al. 2015; Grossman et al. 2006). So far, there is no published study on the effect of La on the plasticity of rat dendritic spines. This study, therefore, explored offspring rats which had just been weaned. Golgi-Cox staining was performed on brain tissue after weaning and changes in dendritic spine density in the CA1 region of the hippocampus were recorded. The results showed that the total density of dendritic spines progressively decreased with the increase in the LaCl₃ dose. The density of mushroom and stubby dendritic spines was significantly reduced in the LaCl₃-treated group; however, the density of thin and branched dendritic spines did not show any change. Mushroom and stubby dendritic spines are mature types of dendritic spines that are closely related to learning and memory. Therefore, it is evident from this study results that La impairs learning and memory by decreasing the total density of dendritic spines hence affecting the density of mature dendritic spines.

The actin cytoskeleton participates in the formation and plasticity of dendritic spines (Penzes and Rafalovich 2012). The actin cytoskeleton regulates the efficiency of synaptic transmission by affecting post-synaptic densities and post-synaptic receptor anchoring. Studies have also confirmed that the dynamic remodeling of the actin cytoskeleton is closely linked to the structural changes of dendritic spines (Yasuda 2017). The Rho GTPase family plays an important role in many biomolecular switches regulating the actin cytoskeleton (Hedrick et al. 2016; Mi et al. 2017). As a core member of Rho GTPases, Rac1 plays a central role in regulating actin cytoskeleton remodeling and affecting dendritic spine plasticity. This occurs in a dynamic process of cycling between activated GTP-bound state and non-activated GDP-bound state (Pyronneau et al. 2017). The principal pathway by which Rac1 regulates actin polymerization involves the phosphorylation/activation of PAK. Rac1 acts to stabilize dendritic spines by promoting the activation of its downstream effector PAK (Chen et al. 2010; Zhang et al. 2005). Activated PAK causes the changes in the expression of Cortactin and Arp2/3 complex hence promoting actin polymerization and remodeling which affects the plasticity of dendritic spines (Wegner et al. 2008). Arp2/3 complex acts as an actin nucleating agent involved in the cytoskeleton of the dendritic pseudopodia (Spence and Kanak 2016). When the complex is activated, new actin filaments are produced on the existing actin filaments and this promotes the formation of actin side branches. In mature dendritic spines, the Arp2/3 complex is remodeled in the actin cytoskeleton which is essential for the plasticity and structural stability of dendritic spines (Kim et al. 2013, 2015). As the regulator of dendritic spine development, Cortactin is highly expressed in the dendritic spines of hippocampal neurons and it affects

the actin cytoskeleton. It also alters the dendritic spine structure by binding to F-actin and Arp2/3 complex (Urano et al. 2001; Weed et al. 2000). In this study, the expression of both Rac1 and GTP-Rac1 showed a declining tendency with an increased dose of LaCl₃ treatment. Besides, the expression of p-PAK, Cortactin, and Arp2/3 complex were down-regulated by La. These results indicated that LaCl₃ inhibited the Rac1/PAK signaling pathway, thereby causing a decrease in the expression of the downstream Cortactin and Arp2/3 complex.

Activity-dependent actin cytoskeleton remodeling in dendritic spines is regulated by CaM kinases in different subtypes of developing and mature neurons. CaMKII is a regulator of glutamatergic synapses which regulates actin cytoskeleton remodeling in dendritic spines by stabilizing actin (Okamoto et al. 2009). Studies have shown that CaMKII causes an increase in the guanine nucleotide exchange factor (GEF) activity of Tiam1 during the formation of dendritic spines thereby activating Rac1 and regulating actin cytoskeleton remodeling (Penzes et al. 2008; Xie et al. 2007). As a Rac1-specific GEF, Tiam1 represents one of the key regulators of dendritic spine development. Studies have shown that Tiam1 is situated in the PSD of dendritic spines, and is important for maintaining dendritic growth, dendritic spine, and synaptic plasticity (Burrell and Li 2008; Tolia et al. 2007). Tiam1 prevents Rac1 activation by interacting with PARD3 in dendritic spines (Tolia et al. 2007). PARD3 recruits Tiam1 to specific sites and this results in space-limited Rac1 activation and local cytoskeleton remodeling (Duman et al. 2013; Mertens et al. 2006). In this study, the results showed that LaCl₃ treatment led to a reduction in the expression of CaMKII, Tiam1, and PARD3. This was an indication that down-regulation of the Rac1/PAK signaling pathway induced by La was associated with the reduced expression of CaMKII, Tiam1, and PARD3.

Rho GTPase activation protein p250GAP negatively regulates dendritic spine plasticity (Nakazawa et al. 2008). In mature neurons, p250GAP interacts with various synapse-specific proteins such as the NMDA receptor, PSD-95, and Fyn, and participates in the regulation of dendritic spine structure-dependent NMDA receptor activity. p250GAP is a target protein for miRNA132 required in dendritic spine formation in the hippocampal neurons (Impey et al. 2010). Previous studies have shown that miRNA132 increases the dendritic spine activity by inhibiting the expression of the Rac1 inhibitor p250GAP, which was at least partially owing to increased dendritic spines. Besides, neuronal activity regulated the dendritic spine production by increasing miRNA132 transcription and activation of the Rac1/PAK signaling pathway (Wayman et al. 2008). Consistent with previous reports, this study found that the expression of p250GAP was negatively correlated with miRNA132 levels in the hippocampus of offspring rats treated with LaCl₃, i.e.,

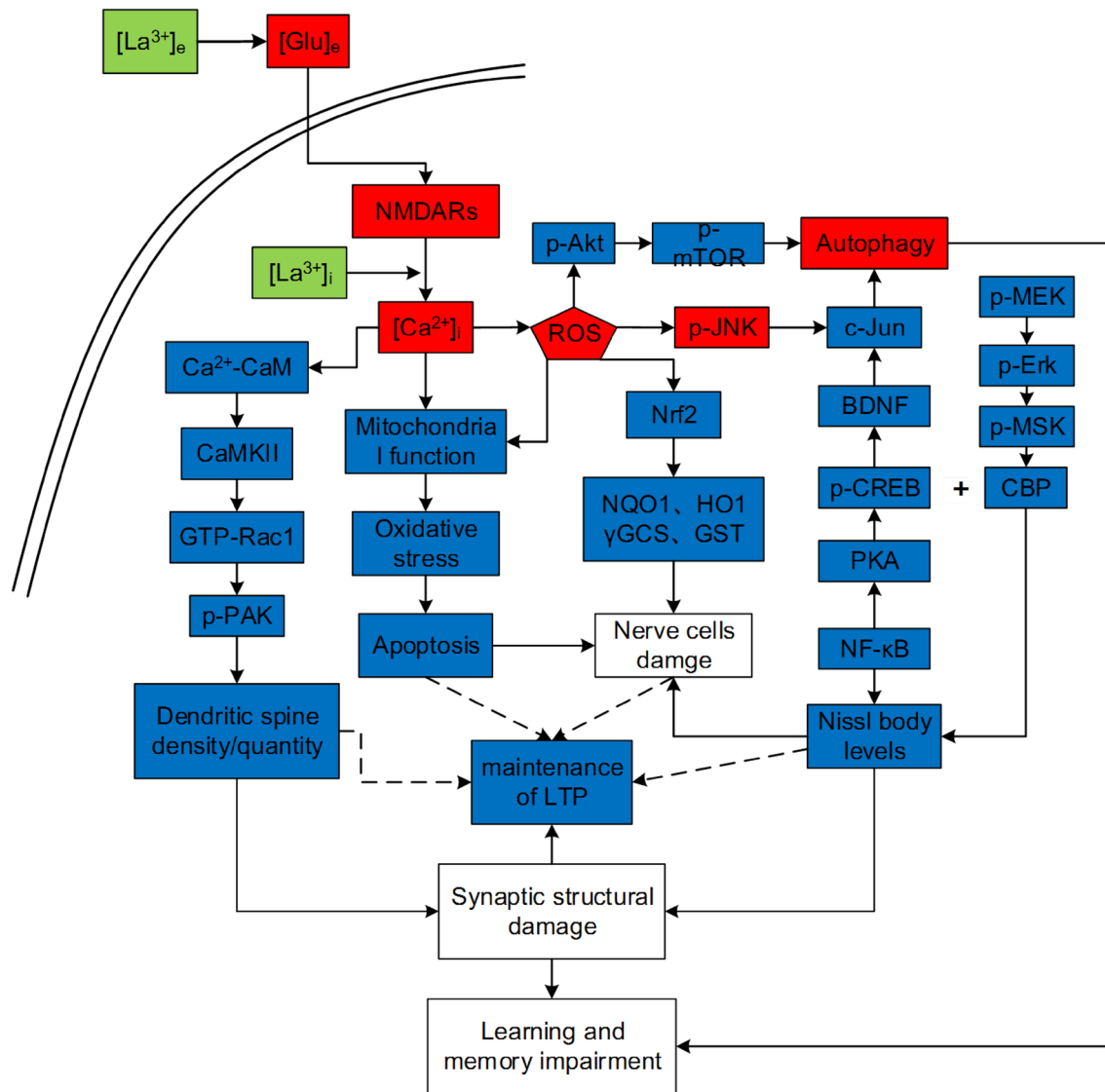


Fig. 8 According to our study, the main signaling pathway involved in La^{3+} entry into hippocampal neurons. See the text for more details. Elements highlighted in red are indicated to be up-regulated/activated/increased, while elements highlighted in blue are indicated to be down-regulated/inhibited/decreased following *in vivo* exposure to La^{3+} . $[\text{La}^{3+}]_e$, extracellular La^{3+} concentration; $[\text{La}^{3+}]_i$, intracellular La^{3+} concentration; $[\text{Ca}^{2+}]_i$, intracellular Ca^{2+} concentration; $[\text{Glu}]_e$, extracellular glutamate concentration; NMDARs, *N*-methyl-D-aspartate receptor; Ca^{2+} -CaM, Ca^{2+} /calmodulin complex; CaMKII, Ca^{2+} /calmodulin-dependent protein Kinase II; Rac1, Ras-associated C3 botulinum substrate; p-PAK, phosphorylated p21-activated kinase; ROS, reactive oxygen species; p-Akt, phosphorylated protein kinase

B; p-mTOR, phosphorylated mammalian target of rapamycin; p-JNK, phosphorylated c-Jun N-terminal kinase; BDNF, brain-derived neurotrophic factor; p-CREB, phosphorylated cAMP response element binding protein; PKA, protein kinase A; NF- κ B, nuclear factor kappa B; p-MEK, mitogen-activated protein kinase kinase; p-Erk, phosphorylated extracellular regulated protein kinase; p-MSK, phosphorylated mitogen and stress-activated protein kinase; CBP, CREB binding protein; Nrf2, nuclear factor erythroid 2-related factor; NQO1, NADP(H): dehydrogenase quinone 1; HO1, heme oxygenase 1; γ GCS, γ -glutamylcysteine synthetase; GST, glutathione s-transferase; LTP, long-term potentiation

the expression of miRNA132 was significantly decreased and that of p250GAP was markedly increased. These results indicate that LaCl_3 -induced down-regulation of Rac1/PAK signaling pathway might involve the abnormal expression of miRNA132 and p250GAP.

The results from existing neurobiology studies indicate that the implementation of learning and memory

functions involves complex regulatory mechanisms bringing together multiple signaling pathways, protein components, and organizational structures. Abnormalities in any of these links can lead to impaired learning and memory. That is, the so-called “pull one hair and you move the whole body.” In order to better understand the cognitive dysfunction caused by La, existing data from the research

group were used to draw a simplified schematic diagram showing the main signal pathway (Fig. 8). Based on this pathway, high intake of La^{3+} leads to Glu accumulation in the synaptic cleft causing NMDA receptor over-activation. This results in the loss of control of the Ca^{2+} channel coupled with the NMDA receptor and leading to a large influx of Ca^{2+} , resulting in $[\text{Ca}^{2+}]_i$ overload (Hu et al. 2018). $[\text{Ca}^{2+}]_i$ overload causes mitochondrial dysfunction and oxidative stress and leads to LTP maintenance disorders (Hu et al. 2018; Wu et al. 2013; Yang et al. 2013). Upregulation of intracellular ROS levels activates ROS-mediated Akt/mTOR and JNK/c-Jun signaling pathways leading to enhanced autophagy and learning and memory dysfunction (Gao et al. 2019; Li et al. 2018; Wang et al. 2019; Zhao et al. 2015). In addition, ROS can also affect the Nrf2 signaling pathway, leading to down-regulation of downstream target genes such as NQO1, HO1, γ GCS, and GST, which causes neuronal damage (Zhang et al. 2017a, b; Zhao et al. 2015). La also down-regulated NF- κ B causing down-regulation of PKA/CREB/BDNF signaling pathway and in turn reduced c-Jun expression levels (Zheng et al. 2013). La down-regulated CBP expression through the MEK/Erk signaling pathway resulting in decreased neuronal Nissl levels and synaptic plasticity disruption, and this affects learning and memory function (He et al. 2008; Liu et al. 2014; Yang et al. 2013). $[\text{La}^{3+}]_i$ accumulated in cells competitively by binding to the CaM domain in the Ca^{2+} -CaM complex, thus causing a decrease in Ca^{2+} -CaM complex (Yang et al. 2013), and decreased CaMKII expression. Down-regulation of the Rac1/PAK signaling pathway causes a decrease in dendritic spine density, which in turn leads to synaptic plasticity disruption and learning and memory dysfunction. Therefore, based on the results of this study and previous reports, we believe that the harmful effects of La in combination with a number of factors impact on the learning and memory.

Conclusion

Based on the above study findings, La causes abnormal expression of Tiam1 and p250GAP which results in down-regulation of the Rac1/PAK signaling pathway and the actin cytoskeleton-related regulatory factors. The above results also indicate that La neurotoxicity affects the learning and memory function and the dendritic spine plasticity as well as density in the hippocampal CA1 neurons of offspring rats.

Acknowledgements This study was supported by the National Natural Science Foundation of China (Nos. 81773469, 81373024, and 81673220).

References

- Allison JE, Boutin C, Carpenter D, Ellis DM, Parsons JL (2015) Cerium chloride heptahydrate ($\text{CeCl}_3 \cdot 7\text{H}_2\text{O}$) induces muscle paralysis in the generalist herbivore, *Melanoplus sanguinipes* (Fabricius) (Orthoptera: Acrididae), fed contaminated plant tissues. *Chemosphere* 120:674–679. <https://doi.org/10.1016/j.chemosphere.2014.09.058>
- Beltran-Campos V, Prado-Alcala RA, Leon-Jacinto U, Aguilar-Vazquez A, Quirarte GL, Ramirez-Amaya V, Diaz-Cintra S (2011) Increase of mushroom spine density in CA1 apical dendrites produced by water maze training is prevented by ovariectomy. *Brain Res* 1369:119–130. <https://doi.org/10.1016/j.brainres.2010.10.105>
- Berry KP, Nedivi E (2017) Spine dynamics: are they all the same? *Neuron* 96:43–55. <https://doi.org/10.1016/j.neuron.2017.08.008>
- Bian WJ, Miao WY, He SJ, Qiu Z, Yu X (2015) Coordinated spine pruning and maturation mediated by inter-spine competition for cadherin/catenin complexes. *Cell* 162:808–822. <https://doi.org/10.1016/j.cell.2015.07.018>
- Burrell BD, Li Q (2008) Co-induction of long-term potentiation and long-term depression at a central synapse in the leech. *Neurobiol Learn Mem* 90:275–279. <https://doi.org/10.1016/j.nlm.2007.11.004>
- Chagnon MJ, Wu CL, Nakazawa T, Yamamoto T, Noda M, Blanchetot C, Tremblay ML (2010) Receptor tyrosine phosphatase sigma (RTPsigma) regulates, p250GAP, a novel substrate that attenuates Rac signaling. *Cell Signal* 22:1626–1633. <https://doi.org/10.1016/j.cellsig.2010.06.001>
- Chen Z-y, Zhu X-d (2008) Accumulation of rare earth elements in bone and its toxicity and potential hazard to health. *J Ecol Rural Environ* 24:88–91
- Chen LY, Rex CS, Babayan AH, Kramar EA, Lynch G, Gall CM, Lauterborn JC (2010) Physiological activation of synaptic Rac > PAK (p-21 activated kinase) signaling is defective in a mouse model of fragile X syndrome. *J Neurosci* 30:10977–10984. <https://doi.org/10.1523/jneurosci.1077-10.2010>
- Chen F et al (2015) Terbium-doped gadolinium oxide nanoparticles prepared by laser ablation in liquid for use as a fluorescence and magnetic resonance imaging dual-modal contrast agent. *Phys Chem Chem Phys* 17:1189–1196. <https://doi.org/10.1039/c4cp04380d>
- Consani S, Balic-Zunic T, Cardinale AM, Sgroi W, Giuli G (2018) A novel synthesis routine for woodwardite and its affinity towards light (La, Ce, Nd) and heavy (Gd and Y). *Rare Earth Elem* 11:150. <https://doi.org/10.3390/ma11010130>
- d'Aquino L et al (2009) Effect of some rare earth elements on the growth and lanthanide accumulation in different *Trichoderma* strains. *Soil Biol Biochem* 41:2406–2413. <https://doi.org/10.1016/j.soilbio.2009.08.012>
- D'Hooge R, De Deyn PP (2001) Applications of the Morris water maze in the study of learning and memory. *Brain Res Brain Res Rev* 36:60–90
- Duman JG, Tzeng CP, Tu YK, Munjal T, Schwechter B, Ho TS, Tolias KF (2013) The adhesion-GPCR BAI1 regulates synaptogenesis by controlling the recruitment of the Par3/Tiam1 polarity complex to synaptic sites. *J Neurosci* 33:6964–6978. <https://doi.org/10.1523/jneurosci.3978-12.2013>
- Dumitriu D, Hao J, Hara Y et al (2010) Selective changes in thin spine density and morphology in monkey prefrontal cortex correlate with aging-related cognitive impairment. *J Neurosci* 30(22):7507–7515. <https://doi.org/10.1523/jneurosci.6410-09.2010>
- Eisenhour D, Reisch F (2006) Industrial minerals and rocks: commodities, markets, and uses. Society for Mining, Metallurgy, and Exploration, Colorado

- Fan G, Yuan Z, Zheng H, Liu Z (2004) Study on the effects of exposure to rare earth elements and health-responses in children aged 7–10 years. *J Hygiene Res* 33:23–28
- Feng L et al (2006) Neurotoxicological consequence of long-term exposure to lanthanum. *Toxicol Lett* 165:112–120. <https://doi.org/10.1016/j.toxlet.2006.02.003>
- Gao X, Yang J, Li Y et al (2019) Lanthanum chloride induces autophagy in rat hippocampus through ROS-mediated JNK and AKT/mTOR signaling pathways. *Metallomics* 11(2):439–453. <https://doi.org/10.1039/c8mt00295a>
- Greenhill SD, Juczewski K, de Haan AM, Seaton G, Fox K, Hardingham NR (2015) NEURODEVELOPMENT. Adult cortical plasticity depends on an early postnatal critical period. *Science* (New York, NY) 349:424–427. <https://doi.org/10.1126/science.aaa8481>
- Grossman AW, Aldridge GM, Weiler IJ, Greenough WT (2006) Local protein synthesis and spine morphogenesis: Fragile X syndrome and beyond. *J Neurosci* 26:7151–7155. <https://doi.org/10.1523/jneurosci.1790-06.2006>
- Gwenzi W, Mangori L, Danha C, Chaukura N, Dunjana N, Sanganyado E (2018) Sources, behaviour, and environmental and human health risks of high-technology rare earth elements as emerging contaminants. *Sci Total Environ* 636:299–313. <https://doi.org/10.1016/j.scitotenv.2018.04.235>
- Haditsch U et al (2009) A central role for the small GTPase Rac1 in hippocampal plasticity and spatial learning and memory. *Mol Cell Neurosci* 41:409–419. <https://doi.org/10.1016/j.mcn.2009.04.005>
- He X, Zhang Z, Zhang H, Zhao Y, Chai Z (2008) Neurotoxicological evaluation of long-term lanthanum chloride exposure in rats. *Toxicol Sci* 103:354–361. <https://doi.org/10.1093/toxsci/kfn046>
- Hedrick NG, Harward SC, Hall CE, Murakoshi H, McNamara JO, Yasuda R (2016) Rho GTPase complementation underlies BDNF-dependent homo- and heterosynaptic plasticity. *Nature* 538:104–108. <https://doi.org/10.1038/nature19784>
- Hu X et al (2018) Lanthanum chloride impairs memory in rats by disturbing the glutamate-glutamine cycle and over-activating NMDA receptors. *Food Chem Toxicol* 113:1–13. <https://doi.org/10.1016/j.fct.2018.01.023>
- Impey S et al (2010) An activity-induced microRNA controls dendritic spine formation by regulating Rac1-PAK signaling. *Mol Cell Neurosci* 43:146–156. <https://doi.org/10.1016/j.mcn.2009.10.005>
- Jiang M et al (2013) Dendritic arborization and spine dynamics are abnormal in the mouse model of MECP2 duplication syndrome. *J Neurosci* 33:19518–19533. <https://doi.org/10.1523/jneurosci.1745-13.2013>
- Joensuu M, Lanoue V, Hotulainen P (2018) Dendritic spine actin cytoskeleton in autism spectrum disorder. *Prog Neuropsychopharmacol Biol Psychiatry* 84:362–381. <https://doi.org/10.1016/j.pnpbp.2017.08.023>
- Kim IH et al (2013) Disruption of Arp2/3 results in asymmetric structural plasticity of dendritic spines and progressive synaptic and behavioral abnormalities. *J Neurosci* 33:6081–6092. <https://doi.org/10.1523/jneurosci.0035-13.2013>
- Kim IH et al (2015) Spine pruning drives antipsychotic-sensitive locomotion via circuit control of striatal dopamine. *Nat Neurosci* 18:883–891. <https://doi.org/10.1038/nn.4015>
- Li JG, Chu J, Pratico D (2018) Downregulation of autophagy by 12/15Lipoxygenase worsens the phenotype of an Alzheimer's disease mouse model with plaques, tangles, and memory impairments. *Mol Psychiatry*. <https://doi.org/10.1038/s41380-018-0268-1>
- Liu H, Yang J, Liu Q et al (2014) Lanthanum chloride impairs spatial memory through ERK/MSK1 signaling pathway of hippocampus in rats. *Neurochem Res* 39(12):2479–2491. <https://doi.org/10.1007/s11064-014-1452-6>
- Luscher C, Nicoll RA, Malenka RC, Muller D (2000) Synaptic plasticity and dynamic modulation of the postsynaptic membrane. *Nat Neurosci* 3:545–550. <https://doi.org/10.1038/75714>
- Mertens AE, Pegtel DM, Collard JG (2006) Tiam1 takes PArT in cell polarity. *Trends Cell Biol* 16:308–316. <https://doi.org/10.1016/j.tcb.2006.04.001>
- Mi Z, Si T, Kapadia K, Li Q, Muma NA (2017) Receptor-stimulated transamination induces activation of Rac1 and Cdc42 and the regulation of dendritic spines. *Neuropharmacology* 117:93–105. <https://doi.org/10.1016/j.neuropharm.2017.01.034>
- Miao L, Ma Y, Xu R, Yan W (2011) Environmental biogeochemical characteristics of rare earth elements in soil and soil-grown plants of the Hetai goldfield, Guangdong Province, China. *Environ Earth Sci* 63:501–511. <https://doi.org/10.1007/s12665-010-0718-9>
- Mleczek P, Borowiak K, Budka A, Niedzielski P (2018) Relationship between concentration of rare earth elements in soil and their distribution in plants growing near a frequented road. *Environ Sci Pollut Res Int*. <https://doi.org/10.1007/s11356-018-2428-x>
- Nakazawa T, Kuriu T, Tezuka T, Umemori H, Okabe S, Yamamoto T (2008) Regulation of dendritic spine morphology by an NMDA receptor-associated Rho GTPase-activating protein, p250GAP. *J Neurochem* 105:1384–1393. <https://doi.org/10.1111/j.1471-4159.2008.05335.x>
- Nishijima H, Ueno T, Funamizu Y, Ueno S, Tomiyama M (2018) Levodopa treatment and dendritic spine pathology. *Mov Disord* 33:877–888. <https://doi.org/10.1002/mds.27172>
- Okamoto K, Bosch M, Hayashi Y (2009) The roles of CaMKII and F-actin in the structural plasticity of dendritic spines: a potential molecular identity of a synaptic tag? *Physiology* (Bethesda, Md) 24:357–366. <https://doi.org/10.1152/physiol.00029.2009>
- Olias M, Ceron JC, Fernandez I, De la Rosa J (2005) Distribution of rare earth elements in an alluvial aquifer affected by acid mine drainage: the Guadiamar aquifer (SW Spain). *Environ Pollut* 135:53–64. <https://doi.org/10.1016/j.envpol.2004.10.014>
- Ota Y, Zanetti AT, Hallock RM (2013) The role of astrocytes in the regulation of synaptic plasticity and memory formation. *Neural Plast* 2013:185463. <https://doi.org/10.1155/2013/185463>
- Penzes P, Rafalovich I (2012) Regulation of the actin cytoskeleton in dendritic spines. *Adv Exp Med Biol* 970:81–95. https://doi.org/10.1007/978-3-7091-0932-8_4
- Penzes P, Cahill ME, Jones KA, Srivastava DP (2008) Convergent CaMK and RacGEF signals control dendritic structure and function. *Trends Cell Biol* 18:405–413. <https://doi.org/10.1016/j.tcb.2008.07.002>
- Penzes P, Cahill ME, Jones KA, VanLeeuwen JE, Woolfrey KM (2011) Dendritic spine pathology in neuropsychiatric disorders. *Nat Neurosci* 14:285–293. <https://doi.org/10.1038/nn.2741>
- Pyronneau A, He Q, Hwang JY (2017) Aberrant Rac1-cofilin signaling mediates defects in dendritic spines, synaptic function, and sensory perception in fragile X syndrome. *Sci Signal* 10:eaan0852. <https://doi.org/10.1126/scisignal.aan0852>
- Rainbow PS (2007) Trace metal bioaccumulation: models, metabolic availability and toxicity. *Environ Int* 33:576–582. <https://doi.org/10.1016/j.envint.2006.05.007>
- Redies C, Hertel N, Hubner CA (2012) Cadherins and neuropsychiatric disorders. *Brain Res* 1470:130–144. <https://doi.org/10.1016/j.brainres.2012.06.020>
- Sala C, Segal M (2014) Dendritic spines: the locus of structural and functional plasticity. *Physiol Rev* 94:141–188. <https://doi.org/10.1152/physrev.00012.2013>
- Spence EF, Kanak DJ (2016) The Arp2/3 complex is essential for distinct stages of spine synapse maturation including synapse silencing. *J Neurosci* 36:9696–9709. <https://doi.org/10.1523/jneurosci.0876-16.2016>
- Spires TL et al (2005) Dendritic spine abnormalities in amyloid precursor protein transgenic mice demonstrated by gene transfer and

- intravital multiphoton microscopy. *J Neurosci* 25:7278–7287. <https://doi.org/10.1523/jneurosci.1879-05.2005>
- Sun Y et al (2018) Lanthanum chloride reduces lactate production in primary culture rat cortical astrocytes and suppresses primary coculture rat cortical astrocyte-neuron lactate transport. *Arch Toxicol* 92:1407–1419. <https://doi.org/10.1007/s00204-017-2148-x>
- Tolias KF, Bikoff JB, Kane CG, Tolias CS, Hu L, Greenberg ME (2007) The Rac1 guanine nucleotide exchange factor Tiam1 mediates EphB receptor-dependent dendritic spine development. *Proc Natl Acad Sci USA* 104:7265–7270. <https://doi.org/10.1073/pnas.0702044104>
- Tsai J, Grutzendler J, Duff K, Gan WB (2004) Fibrillar amyloid deposition leads to local synaptic abnormalities and breakage of neuronal branches. *Nat Neurosci* 7:1181–1183. <https://doi.org/10.1038/nn1335>
- Urano T et al (2001) Activation of Arp2/3 complex-mediated actin polymerization by cortactin. *Nat Cell Biol* 3:259–266. <https://doi.org/10.1038/35060051>
- Wang L, Liang T, Kleinman PJ, Cao H (2011) An experimental study on using rare earth elements to trace phosphorus losses from nonpoint sources. *Chemosphere* 85:1075–1079. <https://doi.org/10.1016/j.chemosphere.2011.07.038>
- Wang B, Wu Q, Lei L et al (2019) Long-term social isolation inhibits autophagy activation, induces postsynaptic dysfunctions and impairs spatial memory. *Exp Neurol* 311:213–224. <https://doi.org/10.1016/j.expneurol.2018.09.009>
- Wayman GA et al (2008) An activity-regulated microRNA controls dendritic plasticity by down-regulating p250GAP. *Proc Natl Acad Sci USA* 105:9093–9098. <https://doi.org/10.1073/pnas.0803072105>
- Weed SA, Karginov AV, Schafer DA, Weaver AM, Kinley AW, Cooper JA, Parsons JT (2000) Cortactin localization to sites of actin assembly in lamellipodia requires interactions with F-actin and the Arp2/3 complex. *J Cell Biol* 151:29–40
- Wegner AM, Nebhan CA, Hu L, Majumdar D, Meier KM, Weaver AM, Webb DJ (2008) N-wasp and the arp2/3 complex are critical regulators of actin in the development of dendritic spines and synapses. *J Biol Chem* 283:15912–15920. <https://doi.org/10.1074/jbc.m801555200>
- Wen B, Liu Y, Hu XY, Shan XQ (2006) Effect of earthworms (*Eisenia fetida*) on the fractionation and bioavailability of rare earth elements in nine Chinese soils. *Chemosphere* 63:1179–1186. <https://doi.org/10.1016/j.chemosphere.2005.09.002>
- Wu J, Yang J, Liu Q, Wu S, Ma H, Cai Y (2013) Lanthanum induced primary neuronal apoptosis through mitochondrial dysfunction modulated by Ca(2)(+) and Bcl-2 family. *Biol Trace Elem Res* 152(1):125–134. <https://doi.org/10.1007/s12011-013-9601-3>
- Xie Z et al (2007) Kalirin-7 controls activity-dependent structural and functional plasticity of dendritic spines. *Neuron* 56:640–656. <https://doi.org/10.1016/j.neuron.2007.10.005>
- Yang J et al (2009) Lanthanum chloride impairs memory, decreases pCaMK IV, pMAPK and pCREB expression of hippocampus in rats. *Toxicol Lett* 190:208–214. <https://doi.org/10.1016/j.toxlet.2009.07.016>
- Yang J, Liu Q, Wu S, Xi Q, Cai Y (2013) Effects of lanthanum chloride on glutamate level, intracellular calcium concentration and caspases expression in the rat hippocampus. *Biometals* 26(1):43–59. <https://doi.org/10.1007/s10534-012-9593-z>
- Yasuda R (2017) Biophysics of biochemical signaling in dendritic spines: implications in synaptic plasticity. *Biophys J* 113:2152–2159. <https://doi.org/10.1016/j.bpj.2017.07.029>
- Zagrebelsky M, Holz A, Dechant G, Barde YA, Bonhoeffer T, Korte M (2005) The p75 neurotrophin receptor negatively modulates dendrite complexity and spine density in hippocampal neurons. *J Neurosci* 25:9989–9999. <https://doi.org/10.1523/jneurosci.2492-05.2005>
- Zhang H, Webb DJ, Asmussen H, Niu S, Horwitz AF (2005) A GIT1/PIX/Rac/PAK signaling module regulates spine morphogenesis and synapse formation through MLC. *J Neurosci* 25:3379–3388. <https://doi.org/10.1523/jneurosci.3553-04.2005>
- Zhang L et al (2017a) The effect of nuclear factor erythroid 2-related factor/antioxidant response element signalling pathway in the lanthanum chloride-induced impairment of learning and memory in rats. *J Neurochem* 140:463–475. <https://doi.org/10.1111/jnc.13895>
- Zhang L et al (2017b) Activation of Nrf2/ARE signaling pathway attenuates lanthanum chloride induced injuries in primary rat astrocytes. *Metallomics* 9:1120–1131. <https://doi.org/10.1039/c7mt00182g>
- Zhao YG, Sun L, Miao G et al (2015) The autophagy gene Wdr45/Wipi4 regulates learning and memory function and axonal homeostasis. *Autophagy* 11(6):881–890. <https://doi.org/10.1080/15548627.2015.1047127>
- Zhao ZH, Zheng G, Wang T et al (2018) Low-level gestational lead exposure alters dendritic spine plasticity in the hippocampus and reduces learning and memory in rats. *Sci Rep* 8(1):3533. <https://doi.org/10.1038/s41598-018-21521-8>
- Zheng L et al (2013) Lanthanum chloride impairs spatial learning and memory and downregulates NF-kappa B signalling pathway in rats. *Arch Toxicol* 87:2105–2117. <https://doi.org/10.1007/s00204-013-1076-7>
- Zhu W, Xu S, Shao P, Zhang H, Wu D, Yang W, Feng J (1997) Bioelectrical activity of the central nervous system among populations in a rare earth element area. *Biol Trace Elem Res* 57:71–77. <https://doi.org/10.1007/bf02803871>
- Zoghbi HY, Bear MF (2012) Synaptic dysfunction in neurodevelopmental disorders associated with autism and intellectual disabilities. *Cold Spring Harb Perspect Biol*. <https://doi.org/10.1101/cshperspect.a009886>

Publisher's Note Springer Nature remains neutral with regard to jurisdictional claims in published maps and institutional affiliations.